

Pin-by-Pin 2D/1D SP3 FDM Scheme with 3D Assembly-wise CMFD Acceleration

Jun Teak Hwang, Namjae Choi, Han Gyu Joo*

Seoul National University, 1 Gwanak-ro, Gwanak-gu, Seoul, 08826, Korea

*Corresponding author: joochan@snu.ac.kr

1. Introduction

Significant advancement in high performance computing technologies has allowed simulating a whole reactor core by directly solving the neutron transport equation. However, even though the processing power has grown rapidly, solving three-dimensional transport equation directly is still infeasible to be performed with reasonable time and resources. As a solution, 2D/1D scheme which treats a 3D system as a synthesis of multiple 2D problems has been suggested. The scheme was first introduced in the DeCART code [1], and to this day, application of 2D/1D scheme into reactor core analysis has been actively studied.

Meanwhile, the technological development also had impacts on the conventional two-step methods. So far, assembly-wise nodal calculations with pin-power reconstruction technique have been employed to analyze light water reactor (LWR) cores. It is still powerful; however, nowadays pin-wise calculation has been able to satisfy the industrial needs in terms of computing time through the computing power advancement. With high-resolution pin-wise homogenized group constants, it can significantly improve the accuracy of the two-step solution over the assembly-wise calculations. As the demand for more accurate core analysis has been recently increased, developments of codes adapting pin-by-pin calculation are proceeding vigorously. For example, SPHINCS [2], performing pin-by-pin SP3 calculation, has been under development in SNU.

The purpose of this paper is to develop an efficient and accurate finite difference method (FDM) scheme based on 3D whole-core solution with pin-homogenized group constants. The 2D/1D approach is applied to FDM, and SP3 equations are solved in both 2D radial (x and y) and 1D axial (z) directions. The details of the method and code implementations are provided in the following sections.

2. Methodology

In this method, a 3D SP3 problem is decomposed into the synthesis of multiple 2D SP3 problems coupled with the axial leakage sources. Axial flux distribution within a plane is reconstructed by 1D SP3 calculation with introducing fine meshes in the plane. Two acceleration techniques are applied: assembly-wise coarse mesh finite difference (CMFD) [3] method and MPI based parallelization.

2.1 2D/1D Decomposed SP3 System

The multi-group formulated SP3 system, including zeroth and second moments, is provided in Eq. (1):

$$\begin{bmatrix} -D_0 \nabla^2 + \Sigma_r & -2\Sigma_r \\ -\frac{2}{3}\Sigma_r & -D_2 \nabla^2 + \frac{4}{3}\Sigma_r + \frac{5}{3}\Sigma_t \end{bmatrix} \begin{bmatrix} \hat{\phi}_0 \\ \phi_2 \end{bmatrix} = \begin{bmatrix} q_0 - TL_0 \\ -\frac{2}{3}q_0 - TL_2 \end{bmatrix} \quad (1)$$

where q_0 represents the fission and scattering source term generated from zeroth flux moment, $\hat{\phi}_0$ is defined as the pseudo zeroth flux ($= \hat{\phi}_0 + 2\phi_2$), and TL is the transverse leakage.

2.2 Axial Transverse Leakage

Axial transverse leakage is reconstructed from the results of 3D assembly-wise CMFD calculation and 1D pin-wise calculation. In order to have a distribution within a coarse mesh, partial current shape (PCS) is applied. The shape is obtained from the result of 1D calculation and denoted as:

$$\omega_{0,i}^{\pm} = \frac{J_{0,i}^{\pm}}{J_0^{\pm}} \quad (2)$$

where i is fine mesh index, J_0^{\pm} is outgoing and incoming partial currents from zeroth moment, and \bar{J}_0^{\pm} is the average partial currents (Eq. (3)).

$$\bar{J}_0^{\pm} = \frac{\sum_{i \in I} J_{0,i}^{\pm} A_{xy,i}}{\sum_{i \in I} A_{xy,i}} \quad (3)$$

In Eq. (3), I represents coarse mesh index, and A_{xy} is the cross-sectional area of the axial pin mesh. By applying the shapes to the partial currents from the CMFD calculation, the pin-wise partial currents for zeroth moment are estimated.

$$J_{0,i}^{\pm} = \omega_{0,i}^{\pm} \bar{J}_{0,I}^{\pm} \quad (4)$$

Then, the net current is calculated using the partial currents to yield the axial transverse leakage, provided in Eq. (5):

$$TL_{0,i} = \frac{(J_{0,i}^{+,Top} - J_{0,i}^{-,Top}) - (J_{0,i}^{+,Bot} - J_{0,i}^{-,Bot})}{H_z} \quad (5)$$

Since CMFD calculation cannot provide the second order current moment, the axial transverse leakage for the second moment is neglected in the 2D calculation.

2.3 Radial Transverse Leakage

The radial transverse leakage is reconstructed from the result of 2D SP3 calculation. Thus, both zeroth and second moment leakage terms can be obtained for the 1D calculation. Eq. (6) describes the average radial leakage for the interested mesh:

$$\bar{L}_i^{xy} = \frac{J_{x,i}^r - J_{x,i}^l}{H_{x,i}} + \frac{J_{y,i}^r - J_{y,i}^l}{H_{y,i}} \quad (6)$$

where superscripts *r* and *l* are right and left surfaces of the mesh, respectively.

The shape of the radial transverse leakage in the plane is approximated by quadratic expansion using the axially neighboring average leakages, as it has been done in the nodal method.

2.4 Iteration Scheme

For 2D and CMFD calculations, biconjugate gradient stabilized method (BiCGSTAB) with incomplete LU preconditioner is applied to solve the linear systems. All operations in the solver are composed of Intel Math Kernel Library (MKL) routines in order to optimize the performance. However, direct solution scheme with block-wise forward and backward substitution is applied to the axial calculation.

Power iteration scheme is applied to 2D and CMFD calculation while 1D calculation is a fixed source calculation. Thus, 1D scheme is only used to provide axial diffusion correction term to the CMFD calculation.

The general calculation scheme is provided in Fig. 1. Noted that the iteration starts with CMFD calculation. In this initial step, the diffusion correction term is set to be zero.

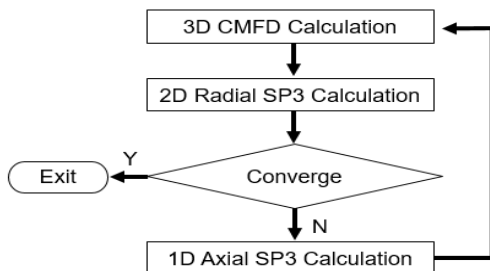


Fig. 1. Calculation scheme of 2D/1D with 3D CMFD acceleration

2.5 MPI Parallelization

Different parallelization strategies are employed for 2D and 1D calculation modules. For 2D calculation, plane-wise axial domain decomposition technique is applied. A certain number of planes are assigned to each processor and independently solved. The parallelization strategy is illustrated in Fig. 2.

However, the plane-wise domain decomposition is difficult to implement for 1D calculation since it is solved directly, which is inherently sequential. Thus, pin-wise radial decomposition is applied (Fig. 3).

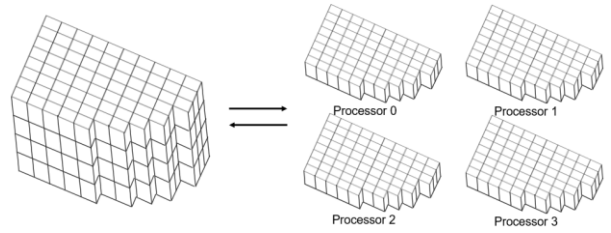


Fig. 2. Plane-wise axial domain decomposition

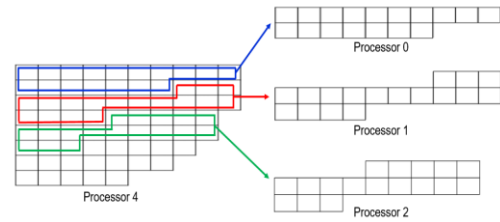


Fig. 3. Pin-wise radial domain decomposition

In this paper, MPI parallelization is not applied to the CMFD calculation since its computational cost is negligible compared to 2D and 1D calculations. The homogenized group constants and diffusion correction terms are calculated on each process and gathered to the master process.

3. Results and Discussion

The performance of the scheme is analyzed in this section. The accuracy is compared with the result of fully 3D FDM. Two problems are tested: C5G7MOX rodged B benchmark problem [4] and modified APR1400 3D core problem. The pin-by-pin group constants are generated from nTRACER [5]. The specifications of the cluster used for calculations are listed in Table 1.

Table 1. Soochiro 4 cluster specification

Nodes	4
CPU	2 × Intel Xeon E5-2630 v4 20 Cores, 2.4 GHz (Boost)
Memory	128GB DDR4 RAM
Interconnect	Infiniband FDR
Compiler	Intel Fortran 17.0.4

3.1 C5G7MOX Rodded B Configuration

Total 9 planes are used and 8 axial sub-meshes are introduced in each plane. Pin-wise two-group constants are used. The axial reflectors containing the control rods are not considered in this case; the group constants for pure water are used instead.

The results are shown in Table 2, when 9 CPU cores are used on single node environment. When the shape function is not applied, assembly-average flat leakage obtained from the CMFD calculation is used. Even though 2D/1D scheme requires more outer iterations for convergence, the total computing time of the scheme is lower than that of fully 3D FDM.

Table 2. Calculation result comparison between 3D and 2D/1D schemes for C5G7MOX rodded B configuration

Scheme	3D	2D/1D	
		Flat	PCS
Shape	-	Flat	PCS
k-eigenvalue	1.07794	1.08237	1.07784
Outer Iterations for Fine Mesh	24	39	96
Outer Iterations for CMFD	306	435	832
Total Computing Times [sec]	1.98	0.35	0.77

Table 3. Accuracy of 2D/1D scheme for C5G7MOX rodded B configuration

Shape	2D/1D	
	Flat	PCS
Radial Max. Abs. Error [%]	2.76	0.85
Radial RMS error [%]	1.29	0.40
Axial Max. Abs. Error [%]	3.47	0.42
Axial RMS error [%]	0.96	0.18

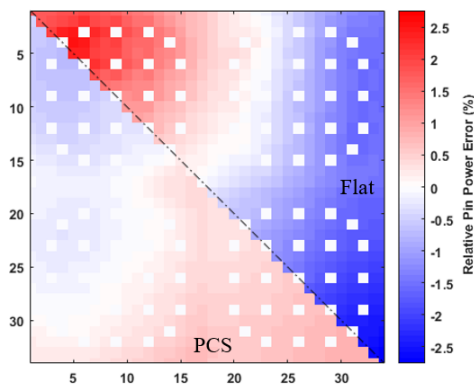


Fig. 4. Relative difference of integrated pin power for C5G7MOX rodded B configuration

The accuracy analysis results are summarized in Table 3. The relative power differences are provided in Fig. 4 and Fig. 5. The application of PCS significantly affects the accuracy. The eigenvalue difference is reduced to 10 pcm from the reference calculation. The

shape application also decreased the root mean square (RMS) errors for both axial and radial direction less than 0.5%.

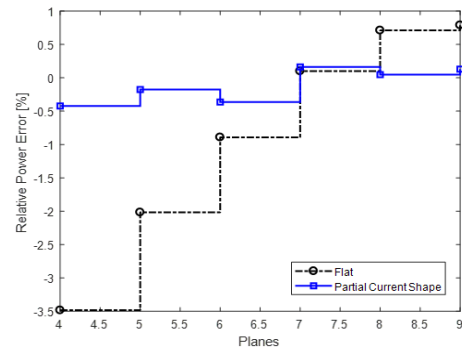


Fig. 5. Relative axial power error distribution for C5G7MOX rodded B configuration

3.2 Modified APR1400 Core Problem

The problem is designed to simulate APR1400 core with the insertion of control rods from regulating group (RG) 5 bank. While 4-group constants are generated based on the nTRACER model for APR1400 [6], the axial blankets on top and bottom positions are neglected.

There are total 27 planes and each plane has a height of 15.24 cm. 6 sub-meshes are introduced into each plane. The rods are inserted 213.36 cm from the top. Total three computer nodes and 27 CPU cores are used.

Table 4 and Table 5 list the overall performance and accuracy, respectively. The integrated relative power differences between fully 3D and 2D/1D schemes are illustrated in Fig. 6 and Fig. 7. In Table 6, values in the parentheses represent the flat distribution on the axial transverse leakage.

Table 4. Calculation result comparison between 3D and 2D/1D schemes for modified APR1400

Scheme	3D	2D/1D	
		Flat	PCS
Shape	-	Flat	PCS
k-eigenvalue	1.00011	1.00016	1.00010
Outer Iterations for Fine Mesh	30	66	66
Outer Iterations for CMFD	1000	2200	2200
Total Computing Times [sec]	25.10	13.32	13.28

Table 5. Accuracy of 2D/1D scheme for modified APR1400

Shape	2D/1D	
	Flat	PCS
Radial Max. Abs. Error [%]	0.47	0.08
Radial RMS error [%]	0.17	0.02
Axial Max. Abs. Error [%]	0.64	0.45
Axial RMS error [%]	0.33	0.32

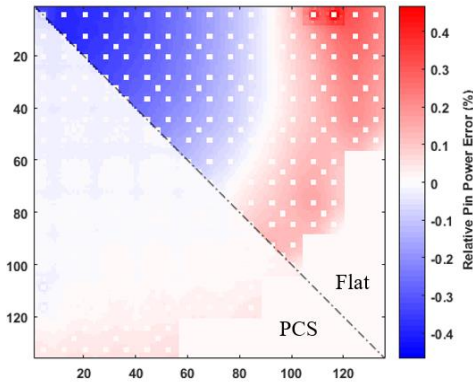


Fig. 6. Relative difference of integrated pin power for modified APR1400

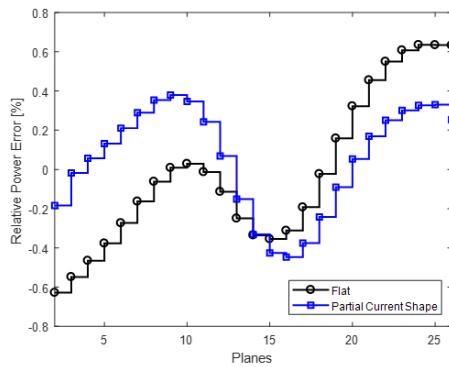


Fig. 7. Relative axial power error distribution for modified APR1400

Table 6. Relative local pin power difference with PCS application

Plane	2	15 (Rod tip)	26
Radial Max. Abs. Error [%]	1.14 (2.78)	0.53 (2.09)	1.28 (3.45)
Radial RMS error [%]	0.13 (0.33)	0.06 (0.28)	0.13 (0.32)

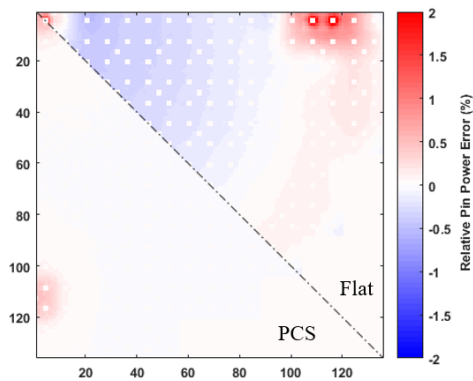


Fig. 8. Relative pin power error at the plane where control rod tips are located (Plane 15)

The application of PCS significantly affects the solutions where the control rod tip is placed and the planes are located adjacent to axial reflectors.

4. Conclusion

Pin-by-pin 2D/1D SP3 FDM scheme with 3D assembly-wise CMFD acceleration has been developed and successfully provide 3D whole core solution.

In the scheme, the 2D radial calculation is followed by the CMFD calculation. Since assembly-averaged currents are obtained from the result of CMFD calculation, some treatments should be introduced to the axial transverse leakage, in order to have a pin-by-pin distribution within the coarse mesh. In this paper, the axial transverse leakage is reconstructed by applying the partial current shape (PCS) obtained from the result of 1D calculation.

Two problems, in which the control rods are partially inserted, are solved. The 2D/1D scheme requires less amount of time to solve both problems than fully 3D scheme while it can produce comparable result as fully 3D FDM. Furthermore, the necessity of a treatment on the axial transverse leakage is also shown. PCS application significantly improves the pin power accuracy of 2D/1D solution; for C5G7MOX rodged B configuration, the radial and axial RMS errors have been reduced to 0.40% and 0.18%, respectively. Moreover, the pin power RMS errors of modified APR1400 core problem are less than 0.32% for both radial and axial directions.

REFERENCES

- [1] H.G. Joo, J.Y. Cho, K.S. Kim, C.C. Lee, S.Q. Zee, Methods and performance of a three-dimensional whole-core transport code DeCART, in: PHYSOR 2004 – The Physics of Fuel Cycles and Advanced Nuclear Systems, Chicago, Illinois, Global Developments, 2004.
- [2] H.H.Cho, et al. Preliminary Development of Simplified P3 based Pin-by-pin Core Simulator, SPHINCS, in: the Korean Nuclear Society Spring, Jeju, 2019
- [3] K. Smith, “Nodal method storage reduction by nonlinear iteration”, Trans. Am. Nucl. Soc. 44 (1983) 265.
- [4] M. A. Smith, et al., “Benchmark on deterministic transport calculations without spatial homogenisation”, NEA/NSC/DOC(2005)16 (2005).
- [5] Y. S. Jung, H. G. Joo et al., “Practical Numerical Reactor Employing Direct Whole Core Neutron Transport and Subchannel thermal/hydraulic solvers”, Annals of Nuclear Energy, Vol. 62, pp. 357-374, 2013.
- [6] H. Hong, H. G. Joo, “Analysis of the APR1400 PWR Initial Core with the nTRACER Direct Whole Core Calculation Code and the McCARD Monte Carlo Code,” Transactions of the Korean Nuclear Society Spring Meeting, Jeju, Korea, May 18-19 (2017).